


REGULAR PAPER

Velocity obstacle–based conflict resolution and recovery method

F. Sun¹, Y. Chen¹ , X. Xu¹, Y. Mu¹ and Z. Wang²

¹Jiangning Road Campus, Nanjing University of Aeronautics and Astronautics, Jiangning District, Nanjing City, Jiangsu Province, China and ²No.1 Jiazi, Changle East Road, Xi'an, Shanxi, China
E-mail: chengyujun7425@nuaa.edu.cn

Received: 28 December 2020; **Revised:** 3 June 2021; **Accepted:** 5 July 2021

Keywords: collision detection and resolution; cooperative game; geometrical algorithm; optimal solution of alliance welfare; particle swarm optimisation algorithm; recovery track; velocity obstacle method

Abstract

Considering the shortcomings of current methods for real-time resolution of two-aircraft flight conflicts, a geometric optimal conflict resolution and recovery method based on the velocity obstacle method for two aircraft and a cooperative conflict resolution method for multiple aircraft are proposed. The conflict type was determined according to the relative position and velocity of the aircraft, and a corresponding conflict mitigation strategy was selected. A resolution manoeuvre and a recovery manoeuvre were performed. On the basis of a two-aircraft conflict resolution model, a multi-aircraft cooperative conflict resolution game was constructed to identify an optimal solution for maximising group welfare. The solution and recovery method is simple and effective, and no new flight conflicts are introduced during track recovery. For multi-aircraft conflict resolution, an equilibrium point that maximises the welfare function of the group was identified, and thus, an optimal strategy for multi-aircraft conflict resolution was obtained.

Nomenclature

V	Spatial scope of the exclusion zone
RCC	The set of relative speeds at which two aircraft collide
VO_{AB}^c	The velocity obstacle cone
l	The distance between the two aircraft
$\Delta\theta$	The change of heading angle
x, y, z	The location of the aircraft
v	The speed of the aircraft
$\alpha, \beta, \gamma, \varepsilon, \varphi, \theta$	The various angles between two aircraft
t	The flight time of the aircraft
$W(j)$	The alliance welfare of strategy combination
S_{safe}	The safety interval of the two aircraft
Q	The fuel consumption
u	The utility function for conflict avoidance

1.0 Introduction

Current implementations of air traffic control (ATC) are typical human-in-the-loop decision-making systems. Because the load that can be placed on controllers is limited and human error is unavoidable, controlling air traffic is difficult, and flight conflicts must be resolved in advance. Conflict detection and resolution (CD&R) is a key technology for air traffic management systems. These systems identify

aircraft encroaching on safe separation limits and provide an efficient resolution scheme; thus, they are crucial for ensuring aircraft flight safety. Constructing effective conflict resolution methods is key for improving these systems [1]. Research in this field is relatively mature, and various methods have been applied to this problem. The artificial potential method [2,3], optimisation algorithm [4,5], optimal control [6–8] and game theory [9,10] are widely used methods. The most widely used method in engineering is the geometric one [11]. This paper describes a CD&R model based on the geometric optimisation method for conflict avoidance applications.

A geometric optimisation approach was proposed by Bilimoria [12] in 2000 and used in the Future Air Traffic Management Concepts Evaluation Tool project [13], but it was used only as an iterative process to solve complex situations. In 2007, Hwang et al. [14] introduced a geometric approach that required shared knowledge of the entire situation. This method undermines autonomous conflict resolution. Several researchers [15,16] have considered the problem of conflict avoidance between two aircraft by using current positions and velocities with geometric and collision cone approaches. Omer and Jérémy [17] modelled the problem by considering the key points of the planned trajectories, including the points at which trajectories intersect. The velocity, acceleration and yaw rate limits were used to solve the indicated conflict and minimise fuel consumption. Some researchers [18–21] have focused on track recovery after resolution, redirecting the aircraft to its original destination without causing new conflicts. However, the turning angle, time and distance of the aircraft are not given, and thus this method is unsuitable.

Geometric approaches involving automated coordination were introduced by Van den Berg et al. [22] in Reciprocal Velocity Obstacles, and then the optimal reciprocal collision avoidance (ORCA) method was proposed in Ref. [23]. Because the velocity obstacle method is simple to implement and geometrically straightforward to understand, it has been commonly applied in UAV autonomous obstacle avoidance methods. The problems of the ORCA method in an ATC context were first demonstrated by Durand et al. [24]. Durand et al. applied a self-separation algorithm used by robots in a flight environment. The position and velocity information of the intruding aircraft was acquired (for example, with ADS-B) to resolve potential flight conflicts. An analytical method based on position and speed was also proposed in Ref. [25,26].

The velocity obstacle method [27–29] is primarily used for autonomous obstacle avoidance in UAV systems. The velocity obstacle method determines the collision probability at a future time by using a geometric model and the relative velocities of the aircraft. The velocity obstacle method defines a relative collision cone (RCC), and when the relative velocity enters this cone, a flight conflict is indicated. To resolve this conflict, the relative velocity is modified to exit the conflict cone along the shortest vector. In this method, aircraft trajectory predictions are based on linear projections of current aircraft states. Linear projections can be computed efficiently and, moreover, prediction errors are negligible during short look-ahead times. However, the method still has the following shortcomings:

- (1) The algorithm is complex, and the step size for changes of aircraft speed and headings is the calculation period.
- (2) If the flight speed is constrained, and if aircraft with similar speeds converge at a small angle, the algorithm tends to choose parallel trajectories for the aircraft that do not approach the destination rather than resolving flight conflicts.

In this study, flight conflict resolution based on the velocity obstacle method was studied in detail with the aim of avoiding numerous speed and direction changes, reducing the number of aircraft manoeuvres, and ensuring flight safety. On the basis of previous work, a geometric model of flight conflict resolution and track recovery was established based on geometric optimisation and minimal manoeuvres (a resolution and a recovery manoeuvre). The model was applied to flight conflicts along a route, and it can reduce the pressure and workload of controllers in practical operation.

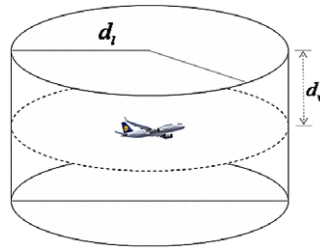


Figure 1. Protection zone.

2.0 Conflict Detection

2.1 Model simplification

According to the characteristics of civil aviation flights and ATC operations, the model is simplified as follows:

- (1) Aircraft are assumed to have the same speed at the beginning of conflict resolution.
- (2) The conflict scenarios studied are restricted to the horizontal plane. Avoidance and recovery manoeuvres can involve changes in aircraft speed, track angle or height.
- (3) The aircraft remains at its ground speed (GS) during climbs and descents.
- (4) Changes in speed or track angle are assumed to be completed in a short time relative to the duration of the overall avoidance or recovery manoeuvre. Hence, for the purpose of this study, these changes in speed or track angle are assumed to occur instantaneously.
- (5) The minimum safety distance between all aircraft must be maintained. Flight separation includes vertical separation of 300 m and horizontal separation of 10 km. Aircraft must maintain at least one of these safety separation distances. For conflict detection purposes, aircraft are assumed to be surrounded by an avoidance region, which is typically a cylinder of radius 10 km and height 300 m. Therefore, a cylinder model was adopted in this study, as shown in Fig. 1.

A conflict is thus defined as the incursion of one aircraft into the exclusion zone of another aircraft. The formula for the exclusion zone in the figure is given by

$$V = \{x^2 + y^2 \leq d_l^2 \cup -d_v \leq z \leq d_v \mid x, y, z \in R\} \tag{1}$$

2.2 Velocity obstacle model

Let AC_1 and AC_2 represent aircraft A and B respectively, let d_l represent the minimum separation distance, and let \vec{v}_1 and \vec{v}_2 represent the velocities of AC_1 and AC_2 , respectively, relative to a ground-based fixed-axis system, as shown in Fig. 2. Therefore, $\vec{v}_R = \vec{v}_1 - \vec{v}_2$ is the relative velocity of AC_1 and AC_2 . α is one-half of the apex angle of the RCC. γ is the angle between \vec{v}_R and AB.

Definition 1. The RCC is the set of $\vec{v}_R = \vec{v}_1 - \vec{v}_2$ such that two aircraft will have a conflict.

$$RCC = \{\vec{v}_R \mid l_{RO} \cap \odot B \neq \emptyset\} \tag{2}$$

l_{RO} is a line colinear with the relative speed vector and $\odot B$ is the exclusion zone about AC_2 .

The model only considers the positional relationship and the current state of the aircraft; if $\vec{v}_R \in RCC$, a conflict will occur; otherwise, no conflicts occur.

Therefore, we can make the following statements regarding flight conflicts between two aircraft:

- If $\alpha > \gamma$, a risk of flight conflict arises;
- If $\alpha < \gamma$, no risk of flight conflict arises.

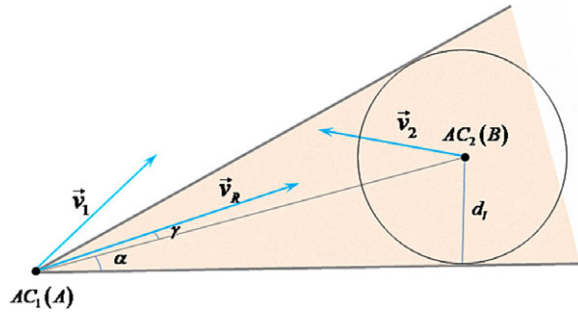


Figure 2. Relative collision cone.

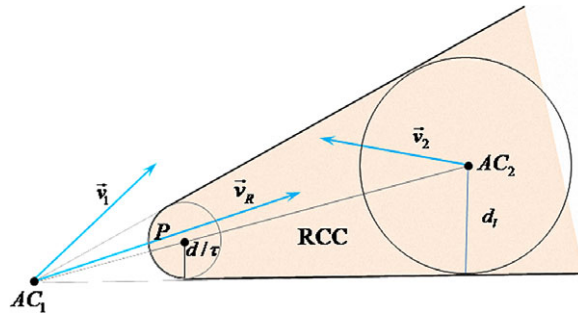


Figure 3. Velocity obstacle model with time constraints.

The values of α and γ can be found by

$$\sin\alpha = \frac{d_1}{\|AB\|} \tag{3}$$

$$\cos\gamma = \cos(\angle(v_R, AB)) = \frac{(v_R \cdot AB)}{\|v_R\| \cdot \|AB\|} \tag{4}$$

2.3 Velocity obstacle model with time constraints

The velocity obstacle model only considers the relationship between the relative speed and the RCC. Any flight conflict between two aircraft in the airspace must be resolved. If the aircraft density in the airspace is high and the velocity obstacle model has no constraints, the number of conflict resolutions undertaken by each aircraft will be too substantial to resolve. Therefore, a time parameter τ was proposed for the velocity obstacle model. That is, a conflict is only identified as such if it will occur within time τ as shown in Fig. 3.

The velocity obstacle cone may be represented as follows:

$$VO_{A/B}^\tau = \{v | \exists t \in [0, \tau] : tv \in \odot B \neq \emptyset\} \tag{5}$$

$\odot P$ is a circular area with $\frac{P_A - P_B}{\tau}$ as the centre and $\frac{r_A + r_B}{\tau}$ as the radius. $\odot B$ is a circular area with $P_A - P_B$ as the centre and $r_A + r_B$ as the radius. $VO_{A/B}^\tau$ is the RCC of AC_1 to AC_2 .

3.0 Conflict Resolution

In this section, we present a conflict resolution and recovery method for two aircraft. Given the position and velocity vectors of the two aircraft, a choice of manoeuvres is presented to the aircraft. Each manoeuvre includes an avoidance segment followed by a recovery segment.

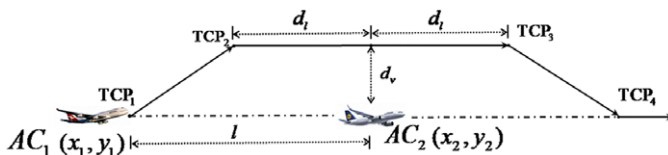


Figure 4. Conflict resolution by altitude change.

3.1 Altitude change (AC)

Let (x_1, y_1) and (x_2, y_2) represent the position coordinates of AC_1 and AC_2 , respectively, relative to the ground-based fixed-axis system, as shown in Fig. 4. Altitude change is adopted for conflict resolution. The aircraft must be separated either horizontally or vertically to avoid entering the exclusion zone during a flight level change. The groundspeed (GS) of the aircraft is assumed to be constant during the manoeuvre. A coordinate system is established with AC_2 as the origin, and the altitude change rate is v_{\perp} .

TCP₁ → TCP₂: The movement of the two aircraft and the safety separation are used to determine the flight track during this stage:

$$\left. \begin{aligned} t_1 &= \frac{d_v}{v_{\perp}} \\ l &= v_R t_1 + d_l \end{aligned} \right\} \Rightarrow l = \frac{d_v \times v_R}{v_{\perp}} + d_l \tag{6}$$

When the distance between AC_1 and AC_2 is l , one aircraft begins to climb (TCP₁) and maintain its altitude (TCP₂) after safe vertical separation has been established between the two aircraft.

TCP₂ → TCP₃: To maintain safe separation between AC_1 and AC_2 at all times, when the separation in the horizontal direction is increasing and has reached d_l , AC_1 begins to descend (TCP₃).

The flight time of AC_1 at this stage is represented as follows:

$$t_2 = 2d_l / v_R \tag{7}$$

TCP₃ → TCP₄: AC_1 descends to its original level at a given rate.

When using the altitude change strategy, the aircraft must maintain a distance of at least l in accordance with the following formula:

$$\sqrt{(x_2 - x_1)^2 + (y_2 - y_1)^2} \geq l \tag{8}$$

Substituting Equation (6) into Equation (8) gives

$$\sqrt{(x_2 - x_1)^2 + (y_2 - y_1)^2} \geq \frac{d_v \times v_R}{v_{\perp}} + d_l \tag{9}$$

3.2 Speed change

3.2.1 Conflict resolution

In Fig. 5, \vec{v}_1 , \vec{v}_2 , and \vec{v}_R are the same as described in Section 2. According to the criterion of the velocity obstacle method, a conflict arises between the two aircraft represented in the figure. In this scenario, a speed change strategy is used such that the new relative speed (\vec{v}'_R) vector direction is the RCC boundary. The speed of AC_2 is constant, and AC_1 accelerates to v'_1 .

During conflict resolution, an inertial coordinate system is established by considering AC_2 to be the origin, and the vector from AC_2 to AC_1 lies on the positive x-axis.

In $\triangle OMN$, the value of v'_1 can be given by the sine theorem:

$$\frac{v'_1}{\sin \varepsilon} = \frac{v_2}{\sin \varphi} \Rightarrow v'_1 = \frac{v_2 \sin \varepsilon}{\sin \varphi} \tag{10}$$

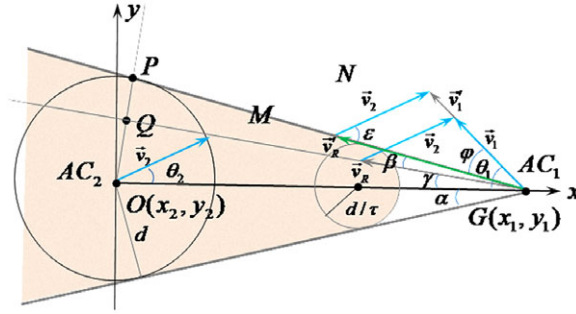


Figure 5. Conflict resolution with flight speed.

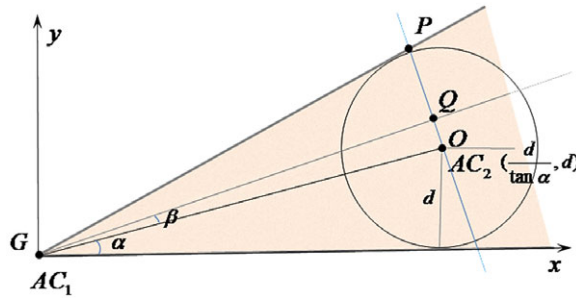


Figure 6. Aircraft position relationships.

In this case, the angle between the aircraft is trivially obtained through algebraic manipulation as follows:

$$\alpha - \beta = \gamma \tag{11}$$

$$\epsilon = \theta_2 + \alpha \tag{12}$$

$$\varphi = \theta_1 - \alpha \tag{13}$$

$$\alpha = \arcsin \frac{d_l}{s} \tag{14}$$

The modified value of \vec{v}_1 is thus as follows:

$$\Delta v_1 = v'_1 - v_1 = \frac{v_2 \sin(\theta_2 + \alpha)}{\sin \varphi} - v_1 \tag{15}$$

The coordinates of AC_1 and AC_2 are (x_1, y_1) and (x_2, y_2) , respectively. Therefore, the distance between the two aircraft is as follows:

$$s = \sqrt{(x_1 - x_2)^2 + (y_1 - y_2)^2} \tag{16}$$

As can be seen from $\|\vec{v}_1\| = \|\vec{v}_2\|$,

$$\theta_1 - \gamma = \theta_2 + \gamma \Rightarrow \gamma = \frac{\theta_1 - \theta_2}{2} \tag{17}$$

To simplify the calculations, the coordinate system is changed, as shown in Fig. 6. AC_2 is located at $(\frac{d}{\tan \alpha}, d)$.

The equations for lines GP , GQ , and PQ are as follows:

$$GP \rightarrow y = \tan(2\alpha)x \tag{18}$$

$$GQ \rightarrow y = \tan(\alpha + \beta)x \tag{19}$$

$$PQ \rightarrow y - d = \tan\left(\frac{\pi}{2} + \alpha + \beta\right)\left(x - \frac{d}{\tan \alpha}\right) \tag{20}$$

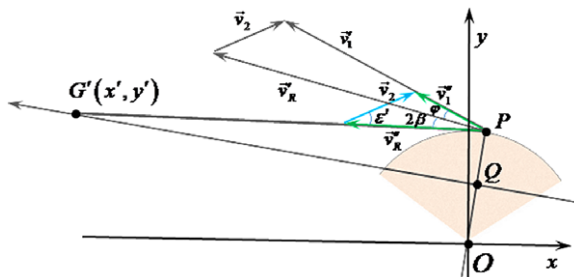


Figure 7. Recovery track and flight speed.

The coordinates of point P can be obtained using Equations (18) and (20):

$$\begin{aligned} \tan(2\alpha) x_p - d &= \tan\left(\frac{\pi}{2} + \alpha + \beta\right) \left(x_p - \frac{d}{\tan \alpha}\right) \\ \Rightarrow [\tan(2\alpha) - \tan\left(\frac{\pi}{2} + \alpha + \beta\right)] x_p &= d - \tan\left(\frac{\pi}{2} + \alpha + \beta\right) \frac{d}{\tan \alpha} \\ \Rightarrow [\tan(2\alpha) + \cot(\alpha + \beta)] x_p &= d + \cot(\alpha + \beta) \frac{d}{\tan \alpha} \\ \Rightarrow x_p &= \frac{d + \cot(\alpha + \beta)}{\tan(2\alpha) + \cot(\alpha + \beta)} \frac{d}{\tan \alpha} \end{aligned} \tag{21}$$

Substituting Equation (21) into either Equation (18) or (20) gives

$$y_p = \tan(2\alpha) \frac{y'_2 + \cot(\alpha + \beta) x'_2}{\tan(2\alpha) + \cot(\alpha + \beta)} \tag{22}$$

3.2.2 Recovery track

After arriving at the track recovery point P, AC₁ decreases its speed, causing the relative velocity to turn toward AC₂ at angle 2β. AC₁ then resumes its original course and flies directly to its destination. The recovery speed is given as follows:

After reaching the track restoration point P, AC₁ turns to the left, causing the relative speed to turn to the left at an angle of 2β. After the relative speed cuts into the original course, AC₁ resumes its original course and flies directly to the destination, as shown in Fig. 7.

$$\frac{v''_1}{\sin \epsilon'} = \frac{v_2}{\sin(\varphi + 2\beta)} \Rightarrow v''_1 = \frac{v_2 \sin \epsilon'}{\sin(\varphi + 2\beta)} \tag{23}$$

$$\epsilon' = \theta_2 + \alpha - 2\beta = \epsilon - 2\beta \tag{24}$$

The modified values of \vec{v}'_1 is given as follows:

$$\Delta v'_1 = v''_1 - v'_1 = \frac{v_2 \sin(\epsilon - 2\beta)}{\sin(\varphi + 2\beta)} - v'_1 \tag{25}$$

In general, aircraft aerodynamic and propulsive considerations constrain the speed manoeuvres that can be executed. Given a speed range of for AC₁, if $v'_1 \in [\underline{v}, \bar{v}]$ and $v''_1 \in [\underline{v}, \bar{v}]$, a speed change strategy can be adopted.

3.3 Heading change

3.3.1 Conflict resolution

Each parameter in the diagram of a conflict displayed in Fig. 8 has the same meaning as those in the previous sections. In this scenario, heading change is used to change the relative speed (\vec{v}'_R) vector to lie on the RCC boundary. AC₂ maintains constant speed, and AC₁ changes its velocity vector to v'_1 .

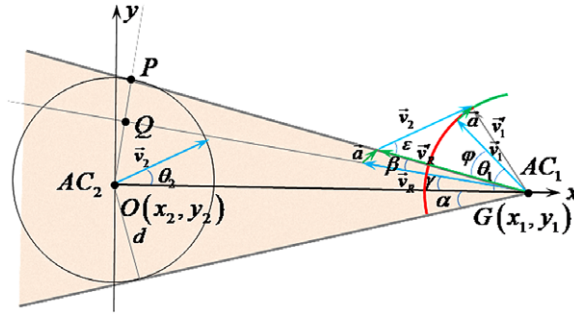


Figure 8. Conflict resolution with flight heading.

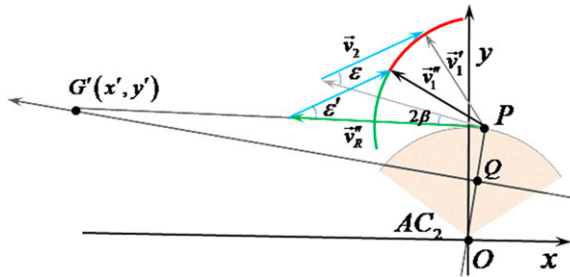


Figure 9. Recovery track with flight heading.

Because the speeds of the two aircraft are initially the same and only the heading of AC₁ changes, the speeds are constant:

$$\|\vec{v}_1\| = \|\vec{v}_2\| = \|\vec{v}'_1\| \tag{26}$$

Assuming that if relative velocity vector is tangent to the RCC boundary, the heading angle of AC₁ changes by Δθ₁, and the change of θ₁ is given as follows:

$$\Delta\theta_1 = \varepsilon - \varphi = \theta_2 - \theta_1 + 2\alpha \tag{27}$$

3.3.2 Recovery track

The direction of the new relative speed vector for the heading change strategy is the same as that for the speed change strategy. Therefore, AC₁ also flies to point P in this case (as described in Section 3.2.1) and will then change course, cut into the original track, and fly to its destination, as shown in Fig. 9.

The heading angle of AC₁ during recovery changes by Δθ'₁:

$$\Delta\theta'_1 = \varepsilon - (\varepsilon' - 2\beta) = 4\beta \tag{28}$$

The angle ε' is given as follows:

$$\varepsilon' = \varepsilon - 2\beta \tag{29}$$

4.0 Conflict Resolution Strategy

During the flight process, three primary types of same-altitude conflicts can arise: same flight path conflicts, cross flight path conflicts, and reverse flight path conflict. Different conflict types have multiple resolution strategies. According to the least cost principle for flight paths, speed resolution is given first priority followed by altitude resolution. Because a change of heading has a higher flight path cost, this strategy is considered last.

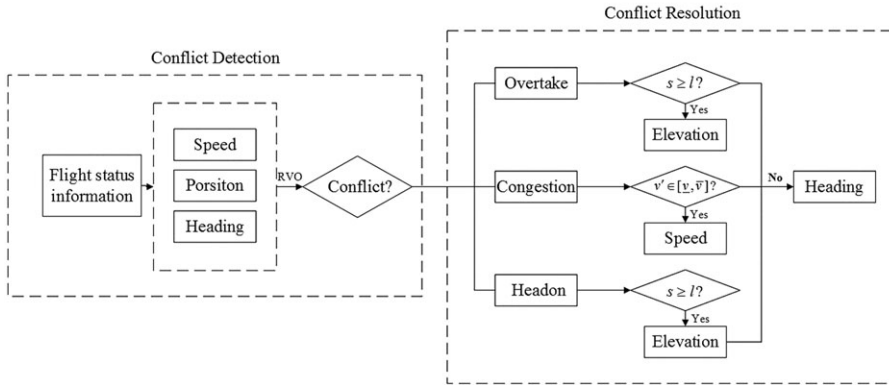


Figure 10. Algorithm flow chart.

The speed resolution strategy is not considered for flight conflicts between aircraft with the same or reverse tracks, and the altitude resolution strategy can only be implemented after certain flight conditions are met. If the conditions for altitude resolution are not met, heading relief can then be used as the conflict resolution option of last resort. A flow chart for resolution selection is shown in Fig. 10.

4.1 Codirectional (0–30°)

Definition 2. A conflict between aircraft with track intersection angles between 0° and 30° is called a codirectional flight conflict.

If the speed of the rear aircraft is greater than that of the front aircraft and the distance between the two aircraft s is greater than the manoeuvre distance l , the rear aircraft can fly over the front aircraft, and thus, altitude change can be used for conflict avoidance.

If $s < l$, heading changes must be used to resolve conflicts. The heading resolution process only involves the use of the speed and position relationships in the x direction:

$$v_{Rx} = v_{1x} - v_{2x} = v_1 \cos \theta_1 - v_2 \cos \theta_2 \tag{30}$$

From Equation (6),

$$l = \frac{d_v \times (v_1 \cos \theta_1 - v_2 \cos \theta_2)}{v_{\perp}} + d_l \tag{31}$$

4.2 Congestion (30°–150°)

Definition 3. A conflict between aircraft with track intersection angles between 30° and 150° is called a cross flight conflict.

If AC_1 can achieve the necessary speed ($v'_1 \leq \bar{v}_1$ and $v''_1 \geq v_1$), speed change can be used to resolve such conflicts.

If AC_1 cannot achieve this speed ($v'_1 > \bar{v}_1$ or $v''_1 < v_1$), heading change can be used to resolve such conflicts.

4.3 Head-on (150°–180°)

Definition 4. A conflict between aircraft with track intersection angles between 150° and 180° is called a reverse trajectory flight conflict.

If $s \geq l$, and there is a conflict of reverse trajectory flight, altitude changes can be used to resolve conflicts.

$$v_{Rx} = v_{1x} - v_{2x} = v_1 \cos \theta_1 - v_2 \cos \theta_2 \quad (32)$$

From Equation (6),

$$l = \frac{d_v \times (v_1 \cos \theta_1 + v_2 \cos \theta_2)}{v_{\perp}} + d_l \quad (33)$$

If $s < l$, heading changes can be used to resolve conflicts.

5.0 Conflict Resolution Strategy for Multi-Aircraft Flights

To extend the aforementioned methods of collision detection and resolution, this section proposes a cooperative game as a model for multi-aircraft conflict resolution. The benefits of all parties are balanced by an optimal solution for group welfare. The conflicting aircraft can cooperate to achieve a small overall deflection angle, thus minimising the cost to the group, meeting fairness requirements, and reducing costs for individual aircraft in a balanced manner according to their importance.

5.1 Cooperative game for conflict resolution

When an aircraft detects that a flight conflict may occur, possible escape strategies of player $I = \{i \mid i \in [1, N]\}$ are applied to form a strategy space S_i , $s_{ij} \in S_i$ where S_{ij} represents the j th strategy of player I , and each player plays against the others (under the constraint of exclusion zones) to achieve a corresponding utility $u = \{u_1, u_2, \dots, u_n\}$. The utility function $u_i: S \rightarrow R$ represents the income of the i th participant under different strategy combinations. The benefits $\{u_1, u_2, \dots, u_n\}$ corresponding to a strategy set $\{s_1, s_2, \dots, s_n\}$ for each player are weighted and summed to obtain the alliance welfare function:

$$W(j) = \sum_i k_i \cdot u_{ij} \quad (34)$$

In the formula, $W(j)$ is the alliance welfare of the j th strategy combination, k_i is a weight coefficient reflecting the importance of an aircraft, and u_{ij} is the payoff of player i under the j th strategy combination. The strategy combination that maximises the welfare function of the alliance is the optimal solution of the cooperative game $\{s_1^*, s_2^*, \dots, s_n^*\}$. The conflict relief process of cooperative game is presented in Fig. 11.

The primary object of study is a group of aircraft that may have dangerous conflicts. Participants have higher utility through group action, but the strategy chosen by an individual aircraft is not necessarily that with the least cost. The optimal solution configuration is that which maximises alliance welfare by ensuring the safety of the group and minimising total avoidance cost. Thus, the aircraft required to perform avoidance manoeuvres and their strategies are determined. Resolution strategies include altitude resolution, speed resolution, and heading resolution. These resolution strategies have different costs, and thus, when the resolution of a multi-aircraft conflict is being investigated, multi-aircraft conflict resolution with minimum cost is the primary topic of study.

The model is simplified as follows with reasonable assumptions based on real-world flight:

- (1) During free flight, except for take-off and landing, aircraft fly at a designated altitude. Therefore, the model can be simplified as a conflict resolution on a two-dimensional plane.
- (2) Owing to safety concerns, nonfighter aircraft do not conduct large-angle manoeuvres, and thus, the change of an aircraft heading angle is within $[-30^\circ, 30^\circ]$. In actual flights, aircraft heading manoeuvres are usually performed in 5° increments. Therefore, changes of the heading angle separated by 5° are included separately in the strategy set.

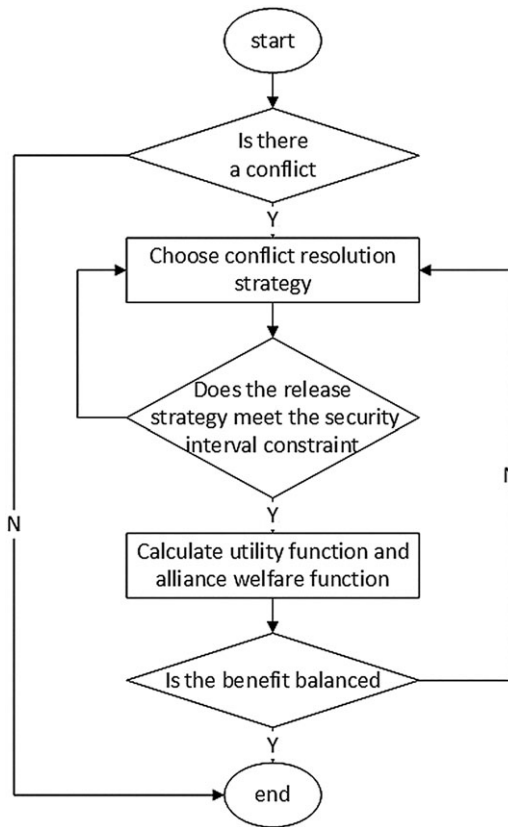


Figure 11. Flow chart of conflict resolution based on cooperative game theory.

- (3) Aircraft are particles, the detection radius of an airborne radar is 100 km, the warning zone is 50 km, and the protection zone is 10 km.

When two aircraft enter each other’s warning zones, a potential threat of flight conflict arises; thus, the resolution process begins. To prevent new conflicts with surrounding aircraft following the resolution of the conflict, all aircraft in the detection range participate in the game to determine a strategy that avoids a second resolution phase. If the distance between two aircraft is less than 10 km, flight conflict occurs and avoidance has failed.

$$S = \sqrt{(x_i - x_j)^2 + (y_i - y_j)^2}, S_{safe} \tag{35}$$

Here, (x_i, y_i) and (x_j, y_j) are the coordinates of aircraft I and j on the plane, respectively, and S_{safe} is the safety interval of 10 km between the two aircraft. The resolution process begins when an aircraft enters the warning area and concludes on leaving the warning area.

5.2 Utility function

The utility function, also known as the payment function, is the utility obtained by participants in the game. In this case, utility represents the avoidance of costs. Aircraft gain higher utility if they have lower manoeuvre costs during conflict resolution, and aircraft that make no manoeuvres therefore have the greatest utility. The utility of each aircraft is investigated for the resolution process. For an individual aircraft, the cost incurred in avoidance is mainly determined by flight range (route fee), flight time, aircraft fuel consumption, and turning angle.

The model assumes that an aircraft flies at cruising speed after entering its route, that its speed does not change during avoidance, and that the range can be expressed as a function of time.

$$S_{\text{total}} = v_{\text{cruise}} \cdot t_{\text{total}} \quad (36)$$

In the formula, S_{total} is the total voyage, v_{cruise} is cruising speed, and t_{total} is the total flight hours.

Because the escape strategies considered are only heading manoeuvres and do not include altitude or speed changes, the fuel consumption can be expressed as a function of the total flight time.

$$Q = \beta t_{\text{total}} \quad (37)$$

Q is fuel consumption and β is the fuel consumption rate, which is determined by aircraft type.

A close relationship exists between the indicators that influence the effectiveness of conflict resolution and flight time. A function of time can be regarded as the utility function in the game, and the corresponding solution is the time-optimal strategy.

$$u_1(t) = \frac{1}{t} \quad (38)$$

In this formula, t is the time from the beginning of the alarm process until the resumption of the route, known as the release time.

The deflection angle of avoidance is also an important index for measuring the avoidance benefit, and the solution strategy maximising to the utility function is the optimal angle strategy.

$$u_2(\theta) = \frac{1}{1 + \sin \theta} \quad (39)$$

In this formula, θ is the aircraft avoidance deflection angle. Higher deflections are more unfavourable for flight safety.

Considering both time and angle, we present a comprehensive utility function for conflict avoidance:

$$u_3(t, \theta) = \frac{1}{\lambda \cdot t(1 + \sin \theta)} \quad (40)$$

In this formula, λ is the adjustment parameter, and a greater λ indicates a greater weight of the time index, whereas a smaller λ represents a greater weight of the deflection angle.

5.3 Conflict resolution based on the particle swarm optimisation algorithm

The particle swarm optimisation (PSO) algorithm begins with a random solution, iterates to an optimal solution, and then makes a fitness evaluation of the solution quality. PSO is easy to implement, has high precision, and has fast convergence; therefore, it is widely used.

In the conflict resolution model of a cooperative game, if the number of conflicting aircraft is large, traversal of all strategy combinations is time-consuming and the requirement of resolution in real time is difficult to meet. The PSO algorithm can be used to solve this problem quickly with the following elements:

- (1) Fitness function: The union welfare function is regarded as the fitness function for the algorithm.
- (2) Coded system: The 13 strategies of $S = \{\theta | \theta = -\frac{\pi}{6} + \frac{\pi}{36} \cdot n, n = 0, 1, \dots, 12\}$ are coded accordingly as strategies 1–13 with $\{x | x \in [1, 13], x \in N\}$.
- (3) Constraint condition: An integer function is used to ensure that the particle position value in each step of the operation is an integer and to ensure safe intervals. $D = \sqrt{(x_i - x_j)^2 + (y_i - y_j)^2} \geq 10$.

A feasible solution is reached by ensuring that the particles are within certain bounds and iterating the position value of particles beyond the boundary. When the position value of the particle is less than

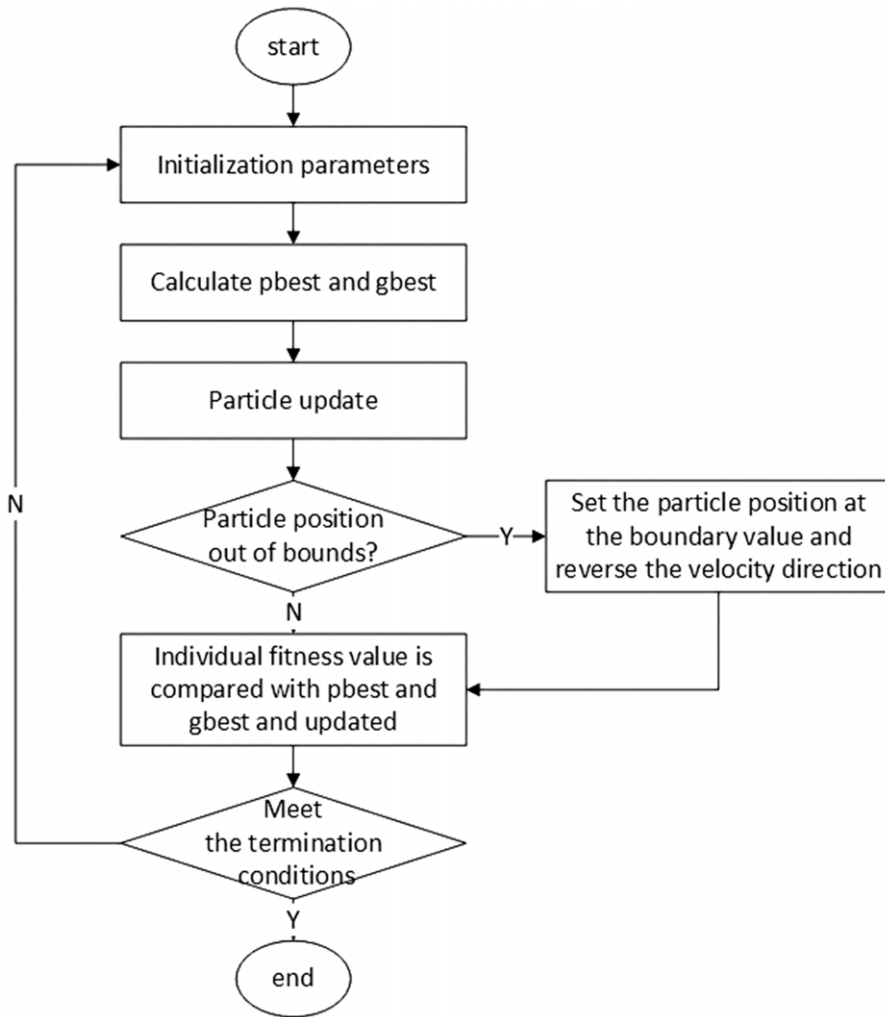


Figure 12. PSO process.

1, the following processing is performed:

$$\begin{cases} p(i,j) = 1 \\ v(i,j) = -v(i,j) \end{cases} \quad (41)$$

Particle position values greater than 13 are treated as follows:

$$\begin{cases} p(i,j) = 13 \\ v(i,j) = -v(i,j) \end{cases} \quad (42)$$

A flow chart of the iterative process is displayed in Fig. 12.

6.0 Simulation and Analysis

6.1 Simulation of collision detection and resolution between two aircraft

Various conflict resolution manoeuvres, as presented in the previous sections, were investigated for specific conflict geometries. To verify the effectiveness of this CD&R strategy, we used MATLAB R2016a

Table 1 Position information

Scenario	Starting point/m	Heading/deg	Speed(km/h)	Time step
1	(0, 200, 4,200)	90	800	0.001
	(110, 200, 4,200)	90	700	
2	(200, 200, 4,200)	90	800	0.001
	(250, 200, 4,200)	270	800	
3	(0, 60, 4,200)	90	750	0.001
	(60, 0, 4,200)	0	750	
4	(0, 100, 4,200)	60	750	0.02
	(100, 0, 4,200)	30	750	

Table 2 Strategy selection

Scenario	Type	Distance		Speed(v'_1)		Judgement	Resolution
		(s)/km	l/km	down	up		
1	Overtake	110	12.78	/	/	$s \geq l$	EC
2	Heading	50	53.25	/	/	$s < l$	HC
3	Congestion	84.85	/	469	1198.4	$v'_1 \notin [600, 900]$	HC
4	Congestion	141.42	/	672.5	836.8	$v'_1 \in [600, 900]$	SC

(Mathworks, MA, USA) to simulate several scenarios. The starting positions of each aircraft were first determined. For example, in Scenario 1, the three-dimensional position coordinate of AC_1 in kilometres was (0, 200, 4.2) with a heading of 90° and speed of 800 km/h. The aircraft is assumed to be in level flight at 4,200 m, and the time constraint is $\tau = 0.05$ h.

According to ATC operation regulations and relevant provisions in the China Civil Aviation Flight Rules, some restrictions on the resolution process were used to ensure applicability to real-world aviation scenarios:

- (1) To ensure the safety and comfort of passengers, a vertical speed of climb and descend is not more than 3 m/s;
- (2) For the speed change resolution strategy, the allowed speeds are [600, 900] km/h.

The simulation was run for test cases to verify the applicability of the methodology. By using the aircraft position and speed information, the conflict type and the utility of various resolution conditions were judged, and then a corresponding conflict resolution strategy was assigned. Table 1 displays the position information for four pairs of aircraft:

For the aircraft position and speed information in each situation presented in Table 1, a determination of the conflict type can be made, and a specific resolution strategy is given. The selection process is presented in Table 2.

Scenario 1:

The first case is an overtake situation where AC_1 and AC_2 are some distance apart and at the same heading. AC_1 begins at (0, 200, 4.2) with a speed of 800 km/h and AC_2 is at (110, 200, 4.2) with a speed of 700 km/h (Fig. 13). During the conflict avoidance process, both aircraft satisfy at least one of the horizontal and vertical separation conditions during both ascent and descent, as required by the process presented in Fig. 11. AC_1 completes the overtaking process and returns to the planned route without causing a new conflict.

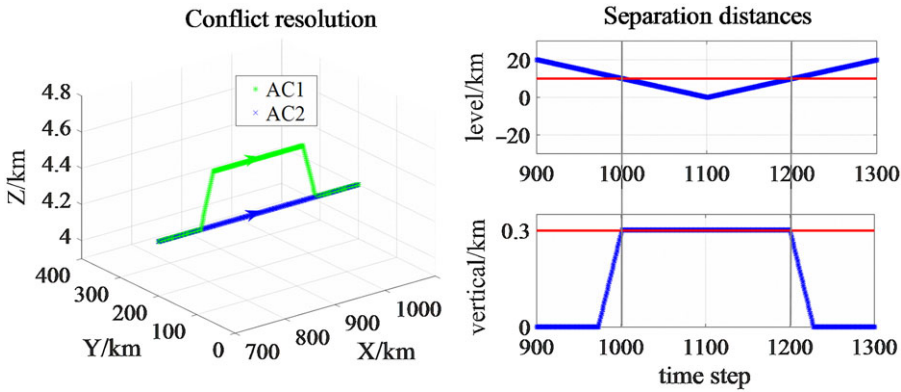


Figure 13. Altitude resolution for an overtake conflict.

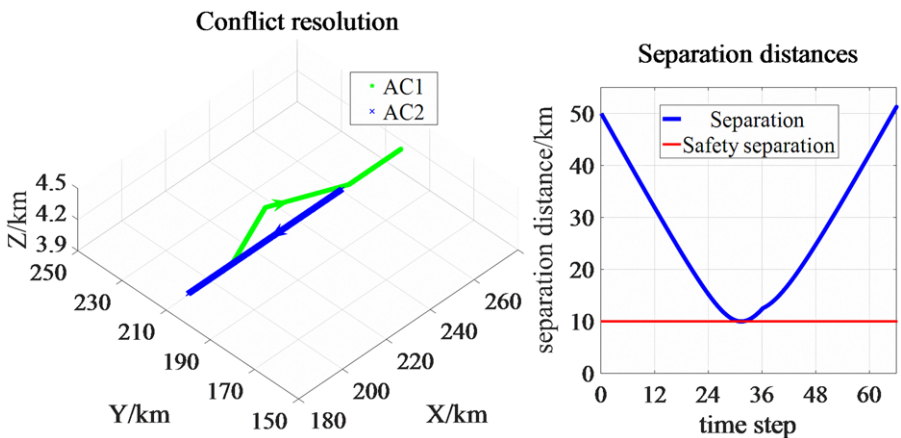


Figure 14. Heading resolution for an overtake conflict.

Scenario 2:

The second case is a heading situation where AC₁ and AC₂ are some distance apart and travelling directly toward each other at the same speed of 800 km/h. AC₁ begins at the origin (200, 200, 4.2) and has a heading of 90°, whereas AC₂ starts at (250, 200, 4.2) and has a heading of 270°, as shown in Fig. 14. Due to insufficient distance for an altitude resolution, a heading change resolution was selected.

Scenario 3:

The third case was a track intersection of 90° with the two aircraft both travelling at 800 km/h. As shown in Fig. 15 AC₁ starts at (0, 60, 4.2) with a heading of 90°, and AC₂ starts at (60, 0, 4.2) with a heading of 0°. A heading change was also chosen for the resolution of this congestion conflict because the required velocity for a speed change resolution was out of bounds (Table 2). The black line on the conflict resolution plot represents the planned track.

Scenario 4:

Figure 16 displays a speed change resolution used for Scenario 4. The speed change can be observed by the position markers for each time step. Note that for AC₁, the speed is substantially higher during resolution, lower during recovery, and then returns to its original value after conflict resolution.

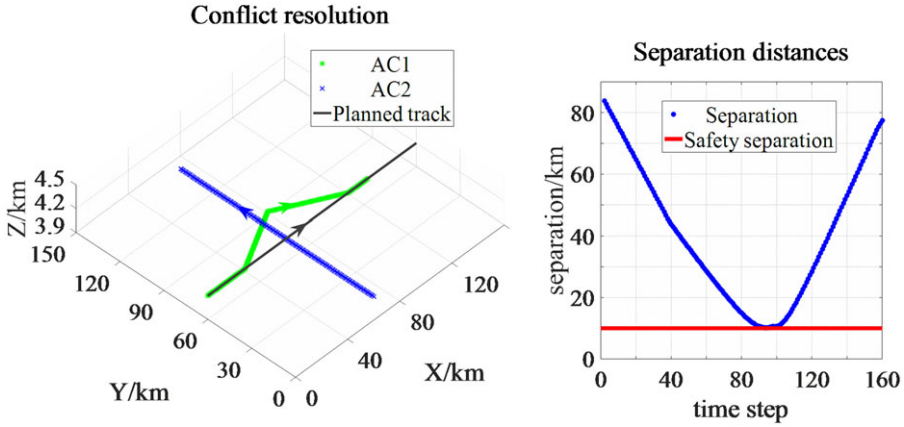


Figure 15. Heading resolution for a 90° intersection conflict.

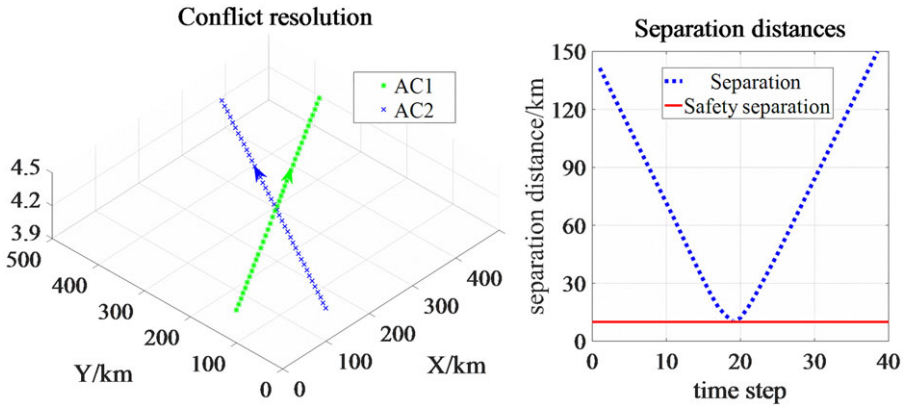


Figure 16. Speed resolution for intersection conflict.

Table 3 Flight state change point

Scenario	CRP/m	TRP/m	COP/m
1	(778.4,2,004,200)	(960.8,2,004,500)	(983.2,2,004,200)
2	(200,200,4200)	(226.5,211.3,4,200)	(253,200,4200)
3	(28.5,604,200)	(68.1,79.7,4,200)	(107.75,604,200)
4	(152.6,188.1,4,200)	(244.7,241.3,4,200)	(347.6,300.7,4,200)

To satisfy ATC requirements, the track points (conflict resolution point [CRP], track recovery point [TRP], and cut-in original track point [COP]) where the flight status changed were also recorded during the simulation (Table 3).

Table 4 displays the change of parameters in each scene during conflict resolution, where Δv_1 , $\Delta v'_1$, and $\Delta \theta_1$, $\Delta \theta'_1$ represent the modified values of the speed and heading for resolution and recovery, respectively, and Δl_1 represents the additional distance travelled by the manoeuvring aircraft (the cost).

In scenarios 2, 3 and 4, the flight level was unchanged, and thus, only the horizontal interval between the two aircraft is given. During these resolutions, AC_1 required two manoeuvres to complete conflict resolution and track recovery, and the horizontal interval between the two aircraft was always greater than 10 km. Because of the introduction of time constraint τ , each pair of aircraft first fly according

Table 4 Comparison of simulation results

Scenario	Δv_1 (km/h)	$\Delta v'_1$ (km/h)	$\Delta \theta_1$ / deg	$\Delta \theta'_1$ / deg	Δl_1 / km
1	/	/	/	/	/
2	/	/	23.1	46.1	35.0
3	/	/	26.4	52.8	26.4
4	86.8	-164.6	/	/	/

Table 5. Turning angle for three different strategies

Aircraft	Strategy		
	Shortest time	Minimum rotation angle	Comprehensive optimisation
a	15°	-15°	-25°
b	15°	-25°	-25°
c	20°	-10°	-10°
d	20°	-5°	-10°
e	25°	-20°	-20°
f	25°	-30°	-20°

to the original route and manoeuvre only when a flight conflict occurs within the time constraint. The aircraft flight course need not be adjusted prematurely, avoiding the excessive occupation of airspace and shortening the time until release.

6.2 Simulation of CD&R for multiple aircraft

To verify flight conflict resolution based on the cooperative game, six-aircraft conflict scenes were simulated in MATLAB. The six-aircraft conflicts were resolved by PSO, and escape routes corresponding to each of the three strategies were obtained. For example, for a resolution using the shortest time strategy was compared with the track obtained by the ergodic method. The validity and stability of the PSO results were verified by the two indexes of operation time and fitness.

In the conflict resolution model for the six-aircraft cooperative game, six players take part: A, B, C, D, E and F. Each aircraft has 13 action choices, including left or right turning of 5°, 10°, 15°, 20°, 25° or 30°, or no manoeuvring. The group welfare functions were W1, W2 and W3, corresponding to aircraft A, B, C, D, E and F located at initial positions (20, 0), (80, 100), (80, 0), (20, 100), (100, 50) and (0, 50), respectively, and flying at 600 km/h.

For the shortest time strategy, the convergence and stability of PSO were tested through comparing the results of the PSO and the ergodic method. The particle population number was $N = 20$, dimension $D = 6$ and iteration times $M = 50$. Because few solutions meet the safety interval requirement, and to improve the ability of the algorithm to leave local optima, a smaller learning factor $c_1 = c_2 = 0.8$ and a larger inertia factor $\bar{w} = 0.8$ were adopted.

From an observation of the changes in the fitness value of the strategy by using convergence algebra, the algorithm was observed to converge to a global optimum value of 0.008 6 in the 41st generation, the convergence was stable, and the run time was substantially reduced. After PSO, the average run time for resolving the six-aircraft conflict was 3.13 s; this approach is therefore suitable for real-time conflict resolution.

The results of the PSO for the shortest time escape strategy, minimum rotation angle escape strategy, and comprehensive optimal strategy are shown in Fig. 17.

The manoeuvring angle of each aircraft at equilibrium for each strategy is shown in Table 5.

The simulation results demonstrate that this method identified effective action choices for a six-aircraft conflict. The action choices obtained for the three utility functions were all in the same direction

Table 6. Turning angle and flight time for different strategies

Aircraft	Strategy		
	Shortest time	Minimum rotation angle	Comprehensive optimisation
a	11/30/	11/20/	11/40/
b	11/30/	11/40/	11/40/
c	11/10/	11/40/	11/20/
d	11/10/	11/30/	11/20/
e	12/00/	11/50/	11/50/
f	12/00/	12/10/	11/50/
Total	69/20/	70/10/	69/40/

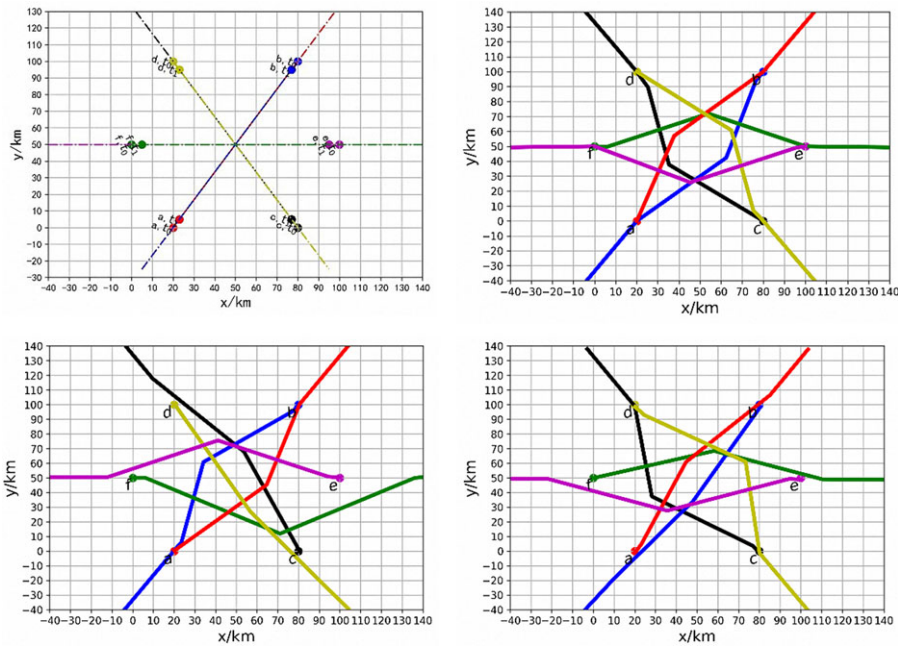


Figure 17. Conflict resolution track based on PSO.

(either all clockwise or all anticlockwise) and therefore were consistent with regulations and command allocation rules. We also compared the flight time of each aircraft under different strategies (Table 6).

The results in Table 6 reveal that the minimum rotation angle strategy increased the flight time somewhat, but the total manoeuvre angle of the group was the smallest. The comprehensive optimal strategy is a compromise strategy based on the two strategies. The avoidance time of each aircraft is within the acceptable range for the optimal strategy. Compared with the genetic algorithm, this algorithm sacrifices some accuracy due to the discretisation of the escape angle, but course changes by 5° intervals more accurately reflect actual flight scenarios, and the additional time and cost required are negligible.

7.0 Conclusions

A method of conflict relief and recovery for flights was proposed. First, the mathematical principles of conflict resolution and track recovery were studied, and the effectiveness of the algorithm was demonstrated. Three strategies of altitude resolution, speed resolution and heading resolution were described in detail. For each conflict resolution strategy used, only one parameter of heading, speed, or altitude

was changed; all aircraft recovered their tracks after resolution. Because the cost of heading resolution is the highest, reducing heading changes could be a focus of further research regarding conflict resolution and recovery strategies for multiple aircraft.

Next, cooperative game theory was applied to the problem, and a cooperative game conflict resolution model was proposed. Group welfare was demonstrated to be a feasible optimal solution for flight conflict problems. Three utility functions were proposed that effectively balance the benefits to all parties and result in a fair set of relief actions that minimise the overall cost to the group. The running time was effectively reduced by using PSO, and hence, real-time CD&R was realised.

Finally, the effectiveness of the method was verified by simulation analysis. The model described is a straightforward and reliable method for detecting and resolving flight conflicts, and it can also be used to identify the track points CRP, TRP and COP.

Acknowledgements. This study was supported by the National Science Foundation of China (No. 71801221).

Supplementary Material. To view supplementary material for this article, please visit <https://doi.org/10.1017/aer.2021.67>

References

- [1] Kuchar, J.K. and Yang, L.C. A review of conflict detection and resolution modeling methods, *IEEE Trans Intell Transport Syst*, 2000, **1**, (4), pp 179–189.
- [2] Zhang, J.Y., Zhao, Z.P. and Liu, T. A path planning method for mobile robot based on artificial potential field, *J Harb Inst Technol*, 2006, **38**, (8), pp 1306–1309.
- [3] Zhang, J.Y. and Liu, T. Optimized path planning of mobile robot based on artificial potential field, *Acta Aeronauticae Astronautica Sinica*, 2007, **28**, (S1), pp 183–188.
- [4] Liu, X., Hu, M.H. and Dong, X.N. Application of genetic algorithms for solving flight conflicts, *J Nanjing Univ Aeronaut Astronaut*, 2002, **34**, (1), pp 35–39.
- [5] Delahaye, D., Peyronne, C., Mongeau, M. and Puechmorel, S. Aircraft conflict resolution by genetic algorithm and B-spline approximation, Proceedings of the 2nd ENRI international workshop on ATM/CNS, Tokyo, Japan, 2010 November 10–12, pp 71–78.
- [6] Chen, L.Y., Han, S.C. and Liu, X. Optimal conflict resolution method based on inner-point restriction, *J Traff Transp Eng*, 2005, **5**, (2), pp 80–84.
- [7] Han, Y.X., Tang, X.M. and Han, S.C. Conflict resolution model of optimal flight for fixation airway, *J Traff Transp Eng*, 2012, **12**, (1), pp 115–120.
- [8] Tang, X.M., Chen, P. and Li, B. Optimal air route flight conflict resolution based on receding horizon control, *Aerosp Sci Technol*, 2016, **50**, pp 77–87.
- [9] Guan, X.M. and Lyu, R.L. Aircraft conflict resolution method based on satisfying game theory, *Acta Aeronauticae Astronautica Sinica*, 2017, **38**, (S1), p 721475.
- [10] Xu, K., Yin, H., Zhang, L. and Xu, Y. Game theory with probabilistic prediction for conflict resolution in air traffic management, 2015 10th International Conference on Intelligent Systems and Knowledge Engineering (ISKE), Taipei, Taiwan, 2015 November, pp 94–98.
- [11] Zhu, C.Y. and Meng, X. Automatic obstacle avoidance algorithm for UAV in dynamic uncertain environment, *J Wuhan Univ Technol (Transp Sci Eng)*, 2013, **37**, (2), pp 307–310.
- [12] Billimoria Karl, D. A geometric optimization approach to aircraft conflict resolution, AIAA Guidance, Navigation, and Control Conference and Exhibit, Reston, VA, AIAA, 2000, pp 14–17.
- [13] Bilimoria, K.D., Sridhar, B., Chatterji, G.B., et al. Facet: Future ATM concepts evaluation tool, Proceedings of the 3rd USA/Europe ATM 2001 R&D Seminar, 2000, p 9.
- [14] Hwang, I., Kim, J. and Tomlin, C. Protocol-based conflict resolution for air traffic control, *ATC Qrtly*, 2007, **15**, (1), pp 1–34.
- [15] Zhang, Y., Zhang, M. and Yu, J. Real-time flight conflict detection and release based on multi-agent system, IOP Conference Series: Earth and Environmental Science, 2018, **108**, (3), p 032053.
- [16] Geser, A. and Munoz, C. A geometric approach to strategic conflict detection and resolution, The 21st Digital Avionics Systems Conference, Irvine, CA, USA, 27–31 October 2002, pp. 6B1–6B1.
- [17] Omer, J. A space-discretized mixed-integer linear model for air-conflict resolution with speed and heading maneuvers, *Comp Oper Res*, 2015, **58**, pp 75–86.
- [18] Goss, J., Rajvanshi, R. and Subbarao, K. Aircraft conflict detection and resolution using mixed geometric and collision cone approaches, AIAA 2004-4879. AIAA Guidance, Navigation, and Control Conference and Exhibit, Providence, Rhode Island, 16–19 August 2004.
- [19] Mueller, T., Schleicher, D. and Bilimoria, K. Conflict detection and resolution with traffic flow constraints, AIAA 2002-4445. AIAA Guidance, Navigation, and Control Conference and Exhibit, Monterey, California, 5–8 August 2002.
- [20] Li, X., Xu, X.H. and Zhu, C.Y. Air traffic reroute planning based on geometry algorithm. *Syst Eng*, 2008, **26**, (8), pp 37–40.

- [21] Zhang, M., Yu, J., Zahng, Y., Wang, S. and Yu, H. Flight conflict resolution during low-altitude rescue operation based on ensemble conflict models, *Adv Mech Eng*, 2017, **9**, (4), p 88–98.
- [22] Van Den Berg, J., Lin, M.C. and Manocha, D. Reciprocal velocity obstacles for real-time multi-agent navigation, 2008 IEEE International Conference on Robotics and Automation, ICRA 2008, Pasadena, California, USA, IEEE, 19–23 May 2008, pp 1928–1935.
- [23] Van Den Berg, J., Guy, S.J., Lin, M. and Manocha, D. *Robotics Research. Springer Tracts in Advanced Robotics*, Berlin, Heidelberg: Springer, 2009, pp 3–19.
- [24] Durand, N. and Barnier, N. Does ATM need centralized coordination? Autonomous conflict resolution analysis in a constrained speed environment, *Air Traffic Control Q*, 2015, **23**, (4), pp 325–346.
- [25] Allignol, C., Barnier, N., Durand, N., Manfredi, G. and Blond, E. Assessing the robustness of a UAS detect & avoid algorithm, 12th USA/Europe Air Traffic Management Research and Development Seminar, Seattle, CA, USA, June 2017.
- [26] Allignol, C., Barnier, N., Durand, N., Manfredi, G. and Blond, E. Integration of UAS in terminal control area, 2016 IEEE/AIAA 35th Digital Avionics Systems Conference (DASC), Sacramento, CA, 12 December 2016, pp 1–7.
- [27] Yang, X.X., Zhou, W.W. and Zhang, Y. Automatic obstacle-avoidance planning for UAV based on velocity obstacle arc method, *Syst Eng Electr*, 2017, **39**, (11), pp 618–176.
- [28] Yang, X.X., Zhang, Y. and Zhou, W.W. Automatic obstacle avoidance algorithm for UAV in dynamic uncertain environment, *Syst Eng Electr*, 2017, **39**, (11), pp 2546–2552.
- [29] Wang, L.L. and Yang, H.D. Rerouting strategy research based on geometry algorithm in flight conflict, *Flight Dynam*, 2012, **30**, (5), pp 466–469.